Superinfections Shape Collective Lysis Dynamics in T-Even Phage Infections: Insights from an Individual-Based Model

Julia Cabrera Cortada[a], Namiko Mitarai[b]

[a] *Department of Animal Welfare and Disease Control, University of Copenhagen, Grønnegårdsvej 8, Frederiksberg, 1870, Denmark*
[b] *The Niels Bohr Institute, University of Copenhagen, Niels Bohr Bygningen, Jagtvej 128, Copenhagen, 2200 N, Denmark*

Abstract

Bacteria cells infected by T-even bacteriophages exhibit a variety of multiplicity of infection (MOI) depenent behaviours: lysis from without (LO) for high number of superinfection, development of resistance against LO (LOR), and lysis inhibition (LIN), a phenomenon in which host cell lysis is delayed when multiple phages infect the same bacterium. We propose an individual-based model that captures these MOI-dependent dynamics phenomenologically. The model assumes a fixed average delay in lysis timing per superinfection, with stochastic variability, and successfully reproduces the experimentally observed multiple peaks in phage production following controlled phage addition. We extend the model to simulate batch culture growth and demonstrate that synchronized collapse of LINed culture can emerge as a collective phenomenon when LOR cells have a higher, but finite, LO threshold. Finally, we apply the model to a spatially structured bacterial colony under phage attack. We find that LO plays a critical role in phage spread due to locally elevated MOI near lysing cells. These results highlight the importance of spatial dynamics and superinfection thresholds in phage-host population outcomes.

Keywords: individual-based modeling, Bacteriophage T4, Lysis inhibition, Superinfection, Phage ecology, Spatial dynamics

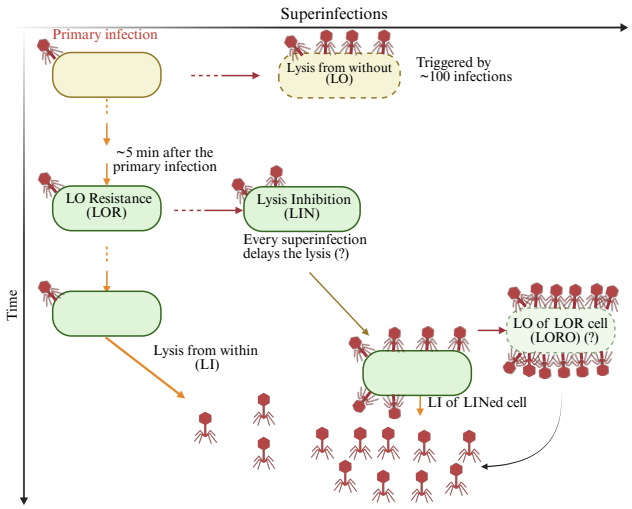

Figure 1: Summary of MOI-dependent behaviors in T-even phages. The vertical axis represents time progression, and the horizontal axis indicates the number of superinfections. Yellow rounded rectangles denote infected cells before LOR is established, while green shapes represent cells that have entered the LOR state. Lysis events triggered by a high number of superinfections (LO or LORO) are indicated by dashed outlines around the corresponding cells. Created in BioRender. Mitarai, N. (2025) https://BioRender.com/j36x932

1. Introduction

Phages are the primary predators of bacteria, shaping microbial ecosystems and driving evolutionary arms races[1]. In marine environments, the phage-to-bacterium ratio often exceeds 1 and can reach up to 100 [2], suggesting that phages frequently face challenges in locating new hosts. This condition increases the likelihood of multiple phages infecting the same bacterium. Moreover, bacteria often grow in colonies or aggregates, further elevating the chance of superinfection, as phages released from a lysed cell are likely to infect neighboring cells [3, 4, 5]. These scenarios make it crucial to understand the consequences of multiplicity of infection (MOI)-dependent interactions in phage-bacteria dynamics.

T-even phages, such as T2 and T4 that infect *Escherichia coli*, exhibit a rich repertoire of MOI-dependent behaviors (see Fig. 1 for an overview and abbreviations). When a bacterium is infected by a large number of phages in rapid succession, it can undergo viron-mediated lysis from without (LO)—a non-productive lysis triggered by damage to the cell envelope caused by phage

tail-associated lysozymes (e.g., gp5 in T4) [6, 7, 8]. However, if the initial infection is not overwhelming, the host cell may establish resistance to LO (LOR) within a few minutes [6, 7]. Once in the LOR state, subsequent superinfections do not cause immediate lysis, but instead trigger lysis inhibition (LIN) [9], extending the latency period before lysis. This extended period can last for several hours and leads to a larger phage yield upon eventual lysis [10].

In liquid cultures with high concentrations of phages and infected cells, cultures undergoing LIN may suddenly clear, as a large number of cells lyse within a short time window. This synchronized burst is known as synchronized lysis inhibition collapse (LINC) [8, 11]. One proposed mechanism for synchronized LINC is that even LOR cells have a finite tolerance to additional infections [11]—once this upper threshold is exceeded, the cell undergoes LO despite its previously established resistance. We refer to this as LO of LOR cells, or LORO.

While the molecular mechanisms underlying these MOI-dependent behaviors have been extensively studied [10, 7, 12, 13, 14, 15], their ecological and population-level consequences are less well understood. Among these, LIN has received the most attention, particularly with respect to its evolutionary advantages [16, 11]. A high MOI suggests a scarcity of uninfected hosts, making it advantageous for a phage to delay lysis and maximize progeny output. In addition, lysis-inhibited cells continue to adsorb and neutralize additional phages, potentially reducing competition from other phage types. These hypotheses have been explored through a mathematical model of phage-bacteria population density dynamics that includes simplified versions of LIN, assuming a single secondary infection induces a fixed delay in lysis [17].

However, we still lack a unified theoretical framework that captures the full spectrum of MOI-dependent behaviors—including LO, LOR, LIN, and LORO—and their effects on phage-bacteria population dynamics. Experimental studies have shown that the number and timing of secondary infections strongly influence the course of LIN. For instance, Bode [18] observed distinct peaks in phage production approximately 5 minutes apart, suggesting that each superinfection adds $\sim$5 minutes of delay and that ongoing superinfection is required to maintain LIN. Capturing such dynamics requires an individual-based model that can track individual cells and their infection histories.

In this study, we develop an individual-based model to investigate MOI-

dependent behaviors of T-even phages. In contrast to population-level models based on density variables, which represent cells infected at different MOIs as distinct subpopulations [19, 20, 17], individual-based models allow direct tracking of each cell's infection history, including the number and timing of superinfections. Our framework incorporates stochastic infection and lysis timing, reproducing the complex dynamics of LIN observed in experiments [18]. We further show that introducing a threshold for LORO can explain synchronized LINC as an emergent collective phenomenon [8, 11]. Finally, we extend the model to a lattice-based spatial environment and demonstrate that local increases in MOI due to phage bursts can trigger LO and LORO in neighboring cells, substantially impacting the survival probability of dense bacterial colonies [21].

2. Model

2.1. individual-based model of T-even phage infection in a well-mixed environment

We model phage–bacteria interactions in a well-mixed liquid culture of volume V. Each bacterium is represented as an individual agent, indexed by $i = 1, 2, \cdots, N$, where N is the total number of bacteria in the system and varies over time due to cell division and lysis. The number of free phage particles, denoted by P, is treated as an integer-valued variable that also changes dynamically through phage adsorption and the release of progeny during lysis events. Each bacterial agent takes a discrete internal state that captures its current infection and growth status. These states encode both the cell's progression through the infection cycle and its MOI- and time-dependent susceptibility to lysis from without (LO), resistance to LO (LOR), lysis from within (LI), lysis inhibition (LIN), and lysis of LOR cell because of too high number of infection (LORO). These states and transitions are described in detail below and summarized schematically in Fig. 2.

Growth of an uninfected cell. We assume that uninfected cells divide with an average growth rate g, incorporating intrinsic stochasticity in division timing. Each cell i is assigned a discrete growth stage variable S_i. When a new cell is born, $S_i = 1$, and it increases incrementally at a constant rate $g \cdot N_g$, where N_g is an integer controlling the variability. The cell with $S_i = N_g$ divides at the rate $g \cdot N_g$. Upon division, two daughter cells are created, each resetting its growth stage variable to 1. This formulation ensures that the mean cell division interval is $1/g$, with $1/\sqrt{N_g}$ coefficient of variation.

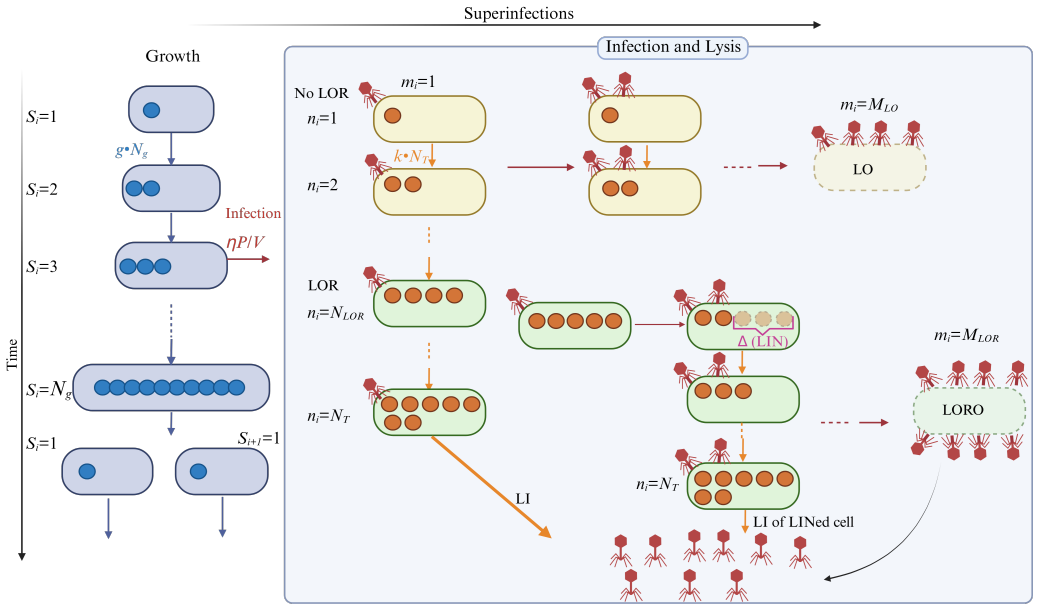

Figure 2: Schematic figure of the individual-based model of T-even phage and host bacteria interaction. See text for the explanation. Created in BioRender. Mitarai, N. (2025) https://BioRender.com/a15g251

Infection stage and lysis. A bacterium becomes infected by a phage at a rate $\eta P/V$, where η is the phage adsorption rate and P is the current number of free phage particles in volume V. Each infection reduces P by one and increases the cell's cumulative infection count m_i by one. Infected cells also track the time since the first infection, t_i, which is used to determine the phage yield upon lysis.

We assume that a minimum time $\tilde{t}$ is required post-infection to produce the first viable phage progeny. After this time, the phage accumulation proceeds linearly at rate α, up to a maximum burstsize β_{max}. Thus, the number of phage progeny in a cell at time t_i is

$$\beta(t_i) = \max(0, \min(\lfloor \alpha \left(t_i - \tilde{t}\right) \rfloor, \beta_{max})). \tag{1}$$

When the cell lyses, $\beta(t_i)$ phages are added to the free phage pool.

We assume that infected cells no longer divide. To regulate the lysis timing depending on superinfection history, a "timer" variable n_i is assigned to each infected cell, which is set to 1 at the first infection and increases incrementally at a rate $k \cdot N_T$ after that. Here, k sets the average latency time, and N_T (an integer) controls timing variability. Without additional infections, the cell undergoes LI when the n_i reaches N_T, corresponding to an average latency time $1/k$ and a coefficient of variation $1/\sqrt{N_T}$. Although the timer variable n_i plays a role reminiscent of holin accumulation in previous models of lysis timing [22], it does not represent an explicit biological entity. In contrast to those models, we do not incorporate gene expression noise; instead, n_i serves purely as a phenomenological construct to control the timing and variability of lysis in a computationally tractable manner.

Superinfection modifies n_i to simulate LIN, but only after LOR has been established. The state transitions are handled as follows:

1. Immediately after the first infection, the cell is susceptible to LO. If m_i, the cumulative number of infections, exceeds the LO threshold M_{LO} before LOR is established, the cell is removed from the system without producing phage progeny.
2. LOR is established when n_i first exceeds the threshold N_{LOR}. This occurs at an average time $N_{LOR}/(k \cdot N_T)$, which is set to be less than $\tilde{t}$, ensuring consistency with the zero-yield assumption of early LO with eq. (1).
3. After LOR is established, each super infection reduces n_i by $\min(n_i - 1, \Delta)$, where Δ (an integer) is a model parameter. The minimum ensures n_i remains positive after the first infection.

4. After LOR, the infected cell can lyse in two ways: (i) Standard lysis: when n_i reaches N_T, making the end of latency (with or without LIN). (ii) LORO-triggered lysis: when the cumulative infections m_i exceed a second threshold M_{LOR} (with $M_{LOR} \geq M_{LO}$). In either case, the cell is removed, and $\beta(t_i)$ phages are released into the environment.

Simulation Algorithm. To efficiently simulate large populations of individuals, we employ the *tau-leaping* method [23], an approximate stochastic simulation algorithm that updates system states over a fixed time step Δt based on the propensity of each event. For additional speed, we perform updates for all bacteria in parallel.

At each simulation step, we assume that there are P free phage particles and N bacterial individuals present in the system at time t. The following steps are performed for all bacteria **without updating** P during the iteration:

A. Phage Infection and Lysis Dynamics:
For each bacterium i, we sample the number of phage adsorption events p_i from a Poisson distribution with mean $\eta P \Delta t / V$. If $p_i > 0$, we execute the following:

(a) Increase the cumulative infection count: $m_i \leftarrow m_i + p_i$.
(b) If this is the first infection of cell i, set the timer: $n_i \leftarrow 1$.
(c) If the cell has not yet established LOR and $m_i \geq M_{LO}$, remove cell i from the system (LO event).
(d) If the cell is in the LOR state:
   i. If $m_i \geq M_{LOR}$, record $p_{\text{new},i} = \beta(t_i)$, remove the cell (LORO event).
   ii. Otherwise, reduce the timer variable:

$$n_i \leftarrow \max(1, n_i - \Delta \cdot p_i)$$

B. Uninfected Cell Growth and Division:
If bacterium i is uninfected, increase its growth stage S_i with probability $g \cdot N_g \cdot \Delta t$. If $S_i = N_g + 1$ after the update, reset $S_i \leftarrow 1$ and record a new cell division.

C. Timer and Lysis Progression for Infected Cells:
For infected cells ($m_i > 0$), increase the timer n_i with probability $k \cdot N_T \cdot \Delta t$. If $n_i = N_T + 1$, record $p_{\text{new},i} = \beta(t_i)$ and remove the cell (LI event).

Final Updates:
After all cells have been processed:

- Update the free phage count:

$$P \leftarrow \max\left(0, P - \sum_i p_i + \sum_i p_{\text{new},i}\right)$$

- Add the recorded number of new cells from step B to the system (each with $S_i = 1$, uninfected).

- Advance the simulation time: $t \leftarrow t + \Delta t$.

This completes one simulation time step. The procedure is repeated until a final simulation time is reached.

Parameters. We fix most parameters to the values found experimentally in phage T4 or T2 infection of *E. coli* growing in a rich medium. The values are summarized in Table 1 with references. In the result section, we vary N_T and Δ, that respectively control the standard deviation of latency time and the latency delay per superinfection, to reproduce the experimental feature found in ref. [18]. We then vary M_{LOR} to be consistent with the synchronized LINC feature reported in ref. [11]. For these parameters, the estimated values are shown in Table 1.

The simulated volume V was $0.01ml$, and the time step Δt was set to be 0.01 min unless otherwise noted to ensure reasonable statistics and computational time.

2.2. Lattice model to simulate spatially structured environment

To investigate the impact of spatial structure, we also developed a one-dimensional lattice model. The system consists of L discrete lattice sites, each of which can host at most one bacterial cell, while multiple phage particles may occupy the same site (Fig. 3).

Phage adsorption occurs when a phage particle shares a site with a bacterium, with an adsorption rate of $\eta_{\text{lattice}} = 200/\text{min}$. This corresponds to a lattice site volume of $v = 10\,\mu\text{m}^3$ when matching a bulk adsorption rate of $\eta = 2 \times 10^{-9}\,\text{ml/min}$. Alternatively, if the site volume is closer to a single cell ($v = 1\,\mu\text{m}^3$), the effective adsorption rate would be ten-fold lower.

Parameter	Description	Default value	Source
g	bacteria doubling rate	$1/30$ min^{-1}	typical fast growth
N_g	growth steps	10	$1/\sqrt{N_g} \sim 30\%$ fluctuation in doubling time
η	phage adsorption rate	2×10^{-9}ml/min	5×10^{-10}ml/min [24] to 5×10^{-9}ml/min [18]
t_0	Eclipse time	15 min	[25, 26]
$1/k$	single infection latency	27 min	[18]. cf. [24, 26]
α	phage production rate	12.5 /min	From single infection burst size 150 [18, 26], cf. [24]
β_{max}	Maximum burst size	500	[25] obtained 400 to 700 phages per LINed cell
M_{LO}	LO threshold	100 phages	[27, 6]
N_T	Threshold for LI	250	Varied to reproduce the fluctuation in [18]
$N_{LOR}/(k \cdot N_T)$	LOR development time	10 min	[6]
N_{LOR}	(model parameter, integer)	92	consistency with above
$\Delta/(k \cdot N_T)$	LIN duration per infection	5 min	Based on [18]
Δ	(model parameter, integer)	46	consistency with above
M_{LOR}	LO threshold for LOR cell	150	Varied to be consistent with the LINC time scale [11]

Table 1: Default parameter for the simulation of well-mixed simulations.

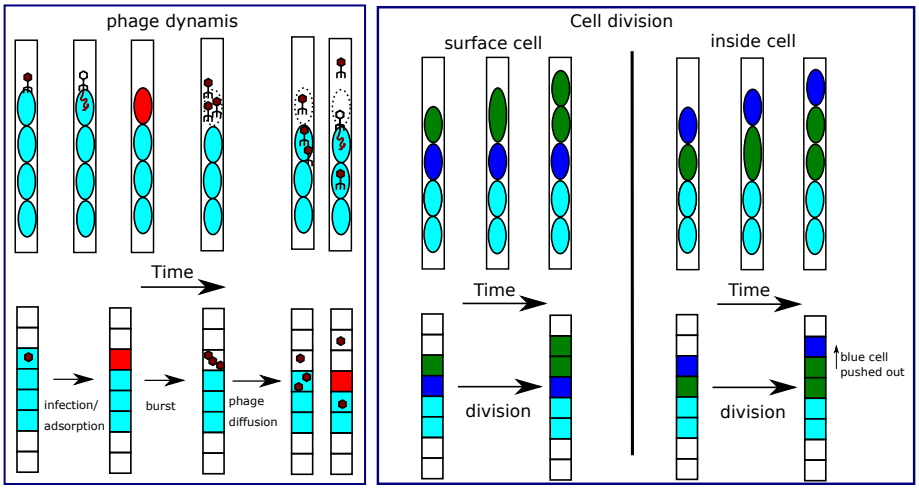

Figure 3: Schematic description of the bacteria division and the phage diffusion and growth in the lattice model. Left: light blue shapes represent uninfected bacteria, red shapes represent infected bacteria, and free phages are represented as brown particles. Right: Cell division and pushing is represented. Different colors are assigned to follow the dividing (green) and pushed (blue) cells.

Phages not undergoing adsorption move via symmetric random walks. Each phage hops to a neighboring lattice site (left or right) at a rate $k_{\text{hop}} = 50/\text{min}$. Assuming a lattice spacing of $1\,\mu\text{m}$, this corresponds to an effective diffusion coefficient consistent with experimental measurements for T4 phage, approximately $D \approx 28\,\mu\text{m}^2/\text{s}$ [28].

Each bacterium's infection dynamics—including responses to superinfection and lysis—follow the same rules as in the well-mixed model described earlier. To simulate bacterial growth, we assume that when an uninfected bacterium divides, all cells between the dividing bacterium and the nearest empty site are displaced one step toward that vacancy (see Fig. 3).

Simulations are run using a fixed time step $\Delta t = 0.004\,\text{min}$, with a lattice size of $L = 300$ sites. At each time step, phage movement by diffusion is updated first. Then, bacterial and infection-related dynamics at each site are updated using random sequential updates: L updates are performed per time step, after which the simulation time is incremented by Δt. We use periodic boundary conditions, but the results are taken before the expanding colony reaches the boundaries and are thus insensitive to the boundary conditions.

2.3. Code availability

All simulation code was written in the Julia programming language and is available at `https://github.com/namikomit/LysisInhibitionAgentBasedModel.git`.

3. Results

3.1. The individual-based model with fixed average delay per superinfection reproduces multiple peaks in phage production time series

We first focus on an informative experiment conducted by Bode *et al.* [18], where *E. coli* cultures at high density were infected by T4 phages at low MOI for a short time, then diluted to avoid further infections. After 15 minutes, the cultures were exposed to a secondary phage input (superinfection) for 3 minutes at varying concentrations. Following this, phages were inactivated or the cultures were diluted again to prevent additional superinfections. Finally, the cultures were continuously filtered through fresh medium, and free phages in the outflow were quantified at about one-minute intervals by plaque assays.

Although the data were somewhat noisy, Bode *et al.* observed that as the superinfection dose increased, phage production over time showed multiple distinct peaks, spaced roughly 5 minutes apart. This suggested that each additional superinfection delayed lysis by approximately 5 minutes, though the exact delay likely depends on the superinfection multiplicity.

To test whether our model can reproduce this phenomenon, we simulated the experimental setup using the following protocol: we initialized the system with 2×10^7 singly infected cells per mL, simulated for 15 minutes, and then added phages at varying concentrations for 3 minutes to induce superinfection. Residual free phages were then removed from the system, and from that point on, we set $\eta = 0$ to prevent further phage adsorption. Rather than modeling the continuous flow of fresh media explicitly, we tracked the number of phages released per minute—analogous to the experimental phage flux.

We first simulated the case without superinfection and compared the resulting time series (normalized to the peak height) with Bode *et al.*'s experimental data. By varying the timer parameter N_T, which controls the stochasticity of lysis timing, we found that $N_T \approx 250$ yielded the best qualitative fit (Fig. 4a). The experimental curve showed a longer tail and slight asymmetry compared to the simulation, but the overall match was reasonable.

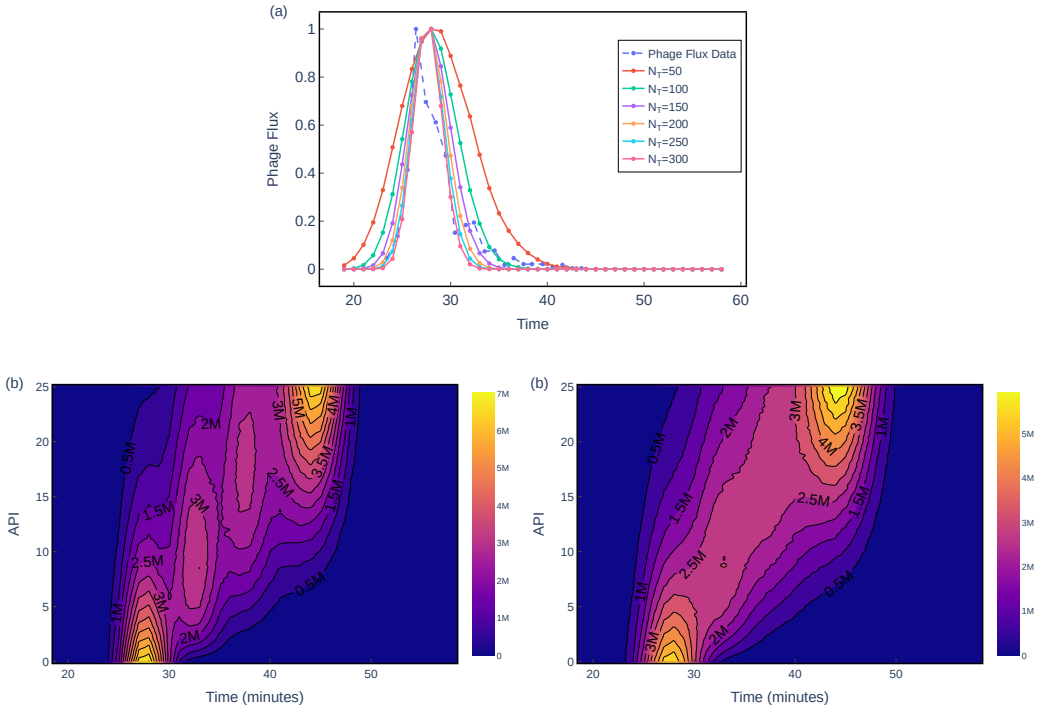

Figure 4: (a) Comparison of phage flux as a function of time. The experimental data was obtained from [18] Fig. 2D. The simulation was done with default parameters as described in the text, except varying the value of the number of timer molecules N_T. All the data are normalized so that the maximum flux becomes 1. (b) Heat map showing the phage produced per min per ml at given time for a given superinfection API for $N_T = 250$. Distinct peaks are observed. (c) The phage flux as a function of time and API when $N_T = 100$, which fails to have distinct peaks.

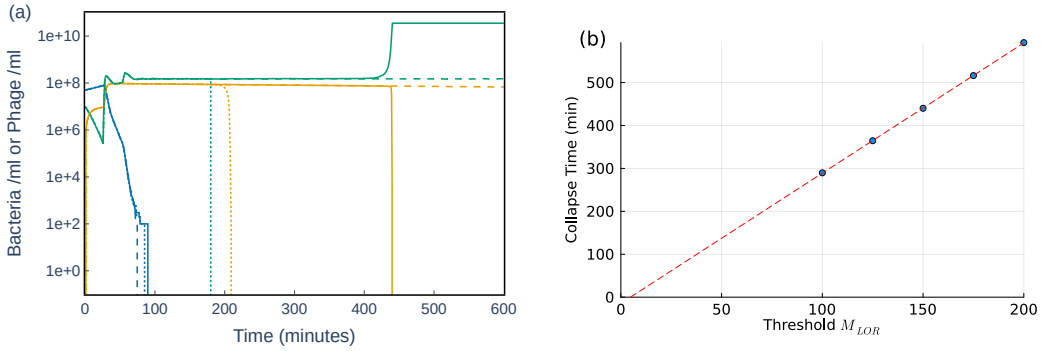

Figure 5: Lysis inhibition collapse simulations. (a)Population dynamics when the LO threshold for LOR cell $M_{LOR} = 150$ (Solid lines) or there is no LO threshold for LOR cell ($M_{LOR} = \infty$, dashed lines). The dotted lines show the case where all the free phages are inactivated after 180 min, emulating the experiment where antiphage agent is added to the culture [8]. Blue: Sensitive bacteria (/ml), Yellow: Infected bacteria (/ml), Green: Free phages (/ml). (b) The population collapse timing as a function of the LO threshold for LINed cell M_{LOR}. Data is shown as filled circles. The dashed line is a linear fit with the slope 3 min per M_{LOR}.

Next, we simulated the superinfection protocol by varying the concentration of phages introduced during the 3-minute secondary infection window. Figure 4b shows the resulting phage flux time series as a function of the average phage input (API), defined as the number of added phages per bacterium during the superinfection phase. We observed multiple distinct peaks, separated by 5 minutes, which progressively shifted to later times as the API increased—qualitatively reproducing the experimental trends.

Finally, we tested the effect of latency time fluctuations by reducing N_T to 150 (Fig. 4c). In this case, the increased stochasticity blurred the peak structure, indicating that small intrinsic variability in lysis timing is crucial for observing well-separated peaks.

3.2. Synchronized lysis inhibition collapse driven by excess superinfection

Next, we simulate batch culture growth of bacteria and phage using LIN parameters determined in the previous section. For simplicity, we assume uninfected bacteria divide with an average doubling time of $1/g = 30$ minutes and a relative standard deviation of approximately 30%. We do not model nutrient limitation, but we ensure that the bacterial population does not exceed 10^9 cells/mL in the simulations presented.

Figure 5a (dashed line) shows the population dynamics in the absence of a lysis threshold for LOR cells—that is, we set $M_{\mathrm{LOR}} = \infty$. In this case, the system reaches a state around 50 minutes where all bacteria become infected, and the population of LINed cells decays very slowly. Meanwhile, the phage concentration fluctuates around a quasi-steady-state value.

This quasi-steady-state phage concentration can be estimated as follows: in our model, each superinfection provides a delay of about $\delta = 5$ minutes in lysis. To maintain the LIN state, each bacterium must be superinfected roughly once every δ minutes, implying an infection rate per cell of $\eta\bar{P} \sim 1/\delta$, where $\bar{P}$ is the mean phage concentration. Using this relation, we estimate $\bar{P} \sim 1/(\delta\eta) = 10^8$ phages/mL. The actual simulation result is slightly higher, $\bar{P} \approx 1.5 \times 10^8$, likely due to fluctuation effects neglected in the estimate.

This stable LIN state is maintained by a negative feedback loop: if phage concentration drops too low to sustain LIN, some infected cells will lyse, releasing phage and restoring the concentration. This creates mild oscillations in phage density and a slow decay of LINed cells.

In reality, however, synchronized collapse of the LIN state—referred to as synchronized LINC—has been observed, with cultures clearing abruptly after a prolonged delay (e.g., ∼5 hours for T4 and ∼8 hours for T2) [8, 11]. Following the suggestion in those studies that LINC may result from excessive superinfection causing lysis even in LOR-established cells, we simulate a finite lysis threshold for LOR by setting $M_{\mathrm{LOR}} = 150$. The resulting dynamics (solid line, Fig. 5a) show an abrupt increase in phage concentration around 400 minutes, followed by a sharp collapse in the bacterial population.

This synchronized collapse is driven by a positive feedback mechanism: once a cell exceeds the infection threshold M_{LOR}, it lyses and releases a large number of phages due to the prolonged LIN-induced production time. These newly released phages then trigger superinfection in other LINed cells, pushing them past their own M_{LOR} threshold. This cascade results in a collective, system-wide collapse.

Interestingly, Abedon [8] also demonstrated that applying an anti-phage agent to inactivate free phages prior to collapse leads to earlier and less synchronized clearing. To reproduce this in silico, we removed all free phages at 180 minutes and disabled further phage production (dotted line, Fig. 5a). In this case, LIN is no longer maintained, and infected cells lyse roughly 5 minutes after phage removal. However, the population decline is gradual rather than abrupt, because there is no positive feedback in this process.

Figure 5b shows how the timing of collapse depends on the value of

M_{LOR}. We observe a clear linear relationship, with collapse time increasing by roughly 3 minutes per unit increase in M_{LOR}. This slope is comparable to the typical time between infections for a LIN-active cell, estimated as $1/(\eta\bar{P}) \sim 2.2$ minutes.

While we lack direct experimental data to determine an appropriate value for M_{LOR}, its effect clearly depends on other parameters such as the adsorption rate η and the phage burst size. For the remainder of this study, we use $M_{\mathrm{LOR}} = 150$, as it is greater than $M_{\mathrm{LO}} = 100$ (Table 1) and produces a biologically reasonable timescale for synchronized LIN collapse given our model parameters.

3.3. Role of the LO, LIN, and LORO in phage attack on a bacterial colony

One natural context where superinfection and secondary infection frequently occur is during phage attack on a densely packed bacterial aggregate or colony. When phages infect cells in such a structure, the progeny released upon lysis are likely to infect neighboring cells at high multiplicity [29, 3, 4, 30, 5, 21].

To study this scenario, we simulate a one-dimensional lattice model in which each site can hold at most one bacterial cell. Phages at a given lattice site can infect the co-localized bacterium, and their infection and lysis responses follow the same rules as in the well-mixed model. Free phages perform a symmetric random walk on the lattice, representing diffusion, and uninfected bacteria divide by pushing adjacent cells toward the nearest empty site (see Section 2.2 for model details and parameters).

Because phages are likely to be adsorbed by surface bacteria when attacking from outside the colony, their ability to penetrate deeply into a dense colony is limited. Prior theoretical work predicts that phage infection reaches only a finite penetration depth γ, beyond which uninfected interior cells may continue to grow [4]. For a one-dimensional system where the bacterial doubling rate is g, the latency time is fixed at τ_l, and phages penetrate to depth γ, the total colony size ℓ evolves as:

$$\frac{d\ell}{dt} = g \ln 2 \cdot (\ell - \gamma) - \frac{\gamma}{\tau_l}, \tag{2}$$

yielding a critical colony size:

$$\ell_c = \left(1 + \frac{1}{\tau_l \cdot g \ln 2}\right)\gamma, \tag{3}$$

above which the colony survives and continues growing despite phage attack. However, this prediction does not incorporate the effects of LO, LIN, or LORO.

Qualitatively, LIN increases the latency time τ_l, thereby lowering ℓ_c and enhancing colony resilience. In contrast, LO and LORO increase bacterial death rates, raising ℓ_c and diminishing survival.

To evaluate these competing effects, we simulate the scenario where a colony of 14 cells is attacked by a single phage on each end, leaving 12 initially uninfected cells. Figure 6(a) shows a spatiotemporal plot, where uninfected and infected cells are visualized over time and space. Upon lysis of the initially infected cells (each releasing 150 phages), the nearest neighbors are likely to experience LO and lyse, while inner cells—fewer phage contacts—can establish LOR. These cells may subsequently enter the LIN state if further infections occur, extending latency and allowing inner uninfected cells to divide.

However, when LINed cells eventually lyse (e.g., due to insufficient superinfection), their large burst size may cause nearby LINed cells to exceed the LOR threshold M_{LOR}, triggering LORO. This creates cascades of synchronized lysis and sharp population drops, visible as large fluctuations in colony size (e.g., around time 80 in Fig. 6a). The right panel shows the number of LO and LORO events per minute, confirming that fluctuations coincide with clustered lysis events from these two mechanisms.

Figures 6(b–f) dissect the roles of each mechanism. Panel (b) removes LIN (by setting $\Delta = 0$), reducing fluctuations but eliminating the protective effect of extended latency. Panels (d) and (f) demonstrate that LIN contributes to protection, while (a) and (c) show that combining LIN with LORO produces large, abrupt fluctuations. Comparing panels (b) and (e) confirms that LO and LORO significantly suppress colony growth.

To quantify these effects, we calculate the long-term survival probability as a function of the initial colony size, assuming two infected cells are placed at the ends. Figure 7 shows that the full model (with LO, LIN, and LORO) requires substantially larger initial colony sizes to achieve survival compared to models omitting LO and LORO. In other words, while LIN alone enhances survival, its protective effects can be overridden by LO and LORO in spatially structured settings. Notably, the model without any of these mechanisms—LO, LORO, or LIN—yields higher colony survival than the full model that includes all three.

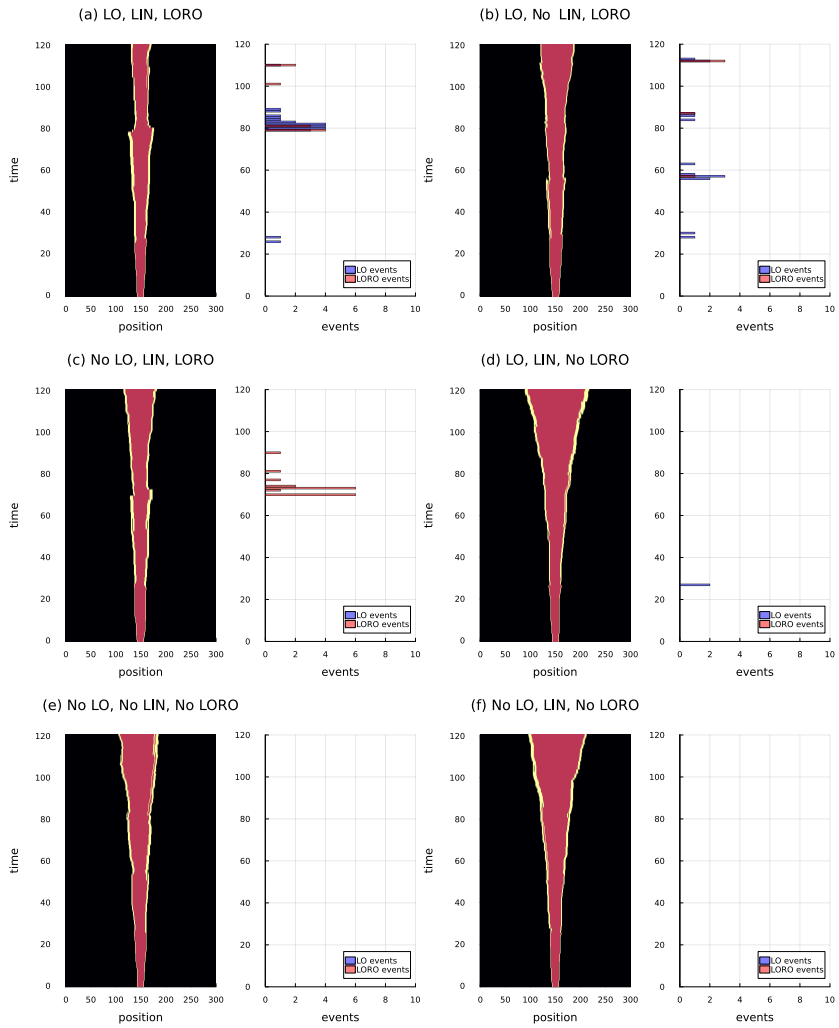

Figure 6: Simulation result of one-dimensional lattice model. (a-f) left: Spatiotemporal plot of the uninfected (red) and infected bacteria (yellow). Initially 12 uninfected bacteria are placed in the middle of the system, and one infected bacteria are placed next to each end of uninfected bacterium. Right: The LO and LORO events per minutes. (a) The full model with LIN and with LO ($M_{LO} = 100$) and with LORO ($M_{LOR} = 150$). (b) The model without LIN, with LO, and with LORO. (c) The model with LIN, without LO ($M_{LO} = \infty$), but with LORO ($M_{LOR} = 150$): In this case, the cells that has not established LOR will burst if the phage infection exceeds M_{LOR} and that is also counted as LORO events. (d) The model with LIN and with LO, and without LORO ($M_{LOR} = \infty$). (e) The model without LI, without LO, and without LORO. (f) The model with LIN, without LO, without LORO.

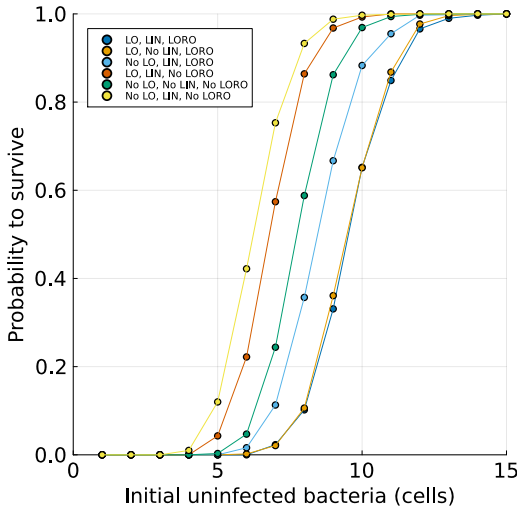

Figure 7: Probability for the colony to keep growing for a given number of uninfected bacteria at the start of the simulation. 1000 samples are taken for each initial condition. Dark blue circle: The full model with LIN and with LO ($M_{LO} = 100$) and with LORO ($M_{LOR} = 150$). Orange circle: The model without LIN, with LO, and with LORO. Light blue circle: The model with LIN, without LO ($M_{LO} = \infty$), but with LORO ($M_{LOR} = 150$): In this case, the cells that has not established LOR will burst if the phage infection exceeds M_{LOR} and that is also counted as LORO events. Red circle: The model with LIN and with LO, and without LORO ($M_{LOR} = \infty$). Green circle: The model without LI, without LO, and without LORO. Yellow circle: The model with LIN, without LO, without LORO.

4. Discussion and conclusion

We have proposed an individual-based model for phage infection and lysis that incorporates fluctuations in lysis timing and MOI-dependent phenomena such as lysis from without (LO), lysis inhibition (LIN), and collapse of LO resistant cells (LORO). When parameters were inferred from existing literature, the model reproduced observed behaviors in well-mixed liquid culture, including multiple peaks in phage production when phages were added at controlled times, as well as synchronized lysis inhibition collapse (LINC) in LINed cultures.

Extending the model to spatially structured environments revealed that LO and LORO can significantly impact colony survival, due to elevated local MOI in neighboring cells following a cell burst. These effects suggest that LO and LORO are important be accounted for when assessing phage spread and bacterial survival in a spatially structured environment.

Recent experiments by Eriksen et al. [21] examined the survival of spherical E. coli colonies embedded in soft agar when challenged with high concentrations of T4 phages, revealing that a relatively large colony size was required for survival. To interpret this observation, a three-dimensional version of the model (Eq. 2) that incorporates nutrient diffusion and consumption was applied. When assuming that the phage latency time is comparable to the bacterial division time, the model estimated a phage penetration depth of approximately 27μm. This is notably deeper than the $\sim$3 μm penetration depth estimate in an earlier study with phage P1vir [31], for which, to our knowledge, LO has not been reported.

Interestingly, Eriksen et al. also found an alternative parameterization for T4 infection, which assumed a latency time approximately nine times shorter and yielded a penetration depth close to 3.5 μm. Although this alternative was deemed biologically implausible due to the unrealistically short latency, our modeling results suggest that the inclusion of LO and LORO effects may help reconcile the observations. Specifically, these effects can accelerate effective killing by allowing a single burst event to lethally affect multiple nearby cells, thereby mimicking the impact of shorter latency times. Thus, LO and LORO may partially explain the observed high rate of killing even under realistic lysis timing assumptions.

However, our current model assumes that dead cells vanish from the system, whereas in reality, cell debris may hinder phage diffusion and adsorption, potentially reducing the efficiency of further infections. Additionally, cell ly-

sis due to LI or LORO likely releases substantial amounts of lysozyme, which may further damage or kill neighboring cells [32]. Neither of these effects was included in the current model, highlighting the need for further refinement to better capture the complex dynamics of T4 infection in dense colonies.

It is important to note that the pronounced effects of LO and LORO in spatially structured simulations depend on the assumption that the thresholds M_{LO} and M_{LORO} are comparable to or lower than the phage burst size β. If these thresholds were significantly higher than β, the frequency of LO or LORO events would be minimal, diminishing their influence.

Assuming that each superinfection induces a $\sim$5-minute delay in LIN, the multiple peaks observed in phage production experiments by Bode [18] imply that the intrinsic fluctuation in lysis timing must be substantially smaller than 5 minutes. Our model fitting suggests a coefficient of variation $1/\sqrt{N_T} \approx 6\%$, corresponding to a standard deviation of approximately 2 minutes for a 27-minute average lysis time. This low level of fluctuation is notable given the complexity of the lysis process [33].

The latency time distribution has been attracting the researchers' interest. Previous single-cell studies of latency time in temperate phage λ showed that fluctuations were only $\sim$5% for a 65-minute average latency between lysogen induction and cell lysis [34]. These results were consistent with a model of holin accumulation governed by stochastic gene expression under fixed gene dosage [22]. For a virulent phage, recent single-cell observations of phage T7 infection report a much larger variation ($\sim$21%) for a 19-minute latency time [35], where a significant portion of the variability was due to differences in duration between adsorption and genome injection. This highlights the need for direct single-cell measurements of T4 lysis timing and LIN response to clarify how tightly T4 infection and lysis are regulated.

Our model's prediction of synchronized LINC (Fig. 5a) features an abrupt collapse in timing, sharper than experimentally observed curves [8, 11]. This discrepancy likely arises because our model assumes uniform parameters across all cells. In reality, variability in cell properties, such as cell size and receptor number, would lead to cell-to-cell heterogeneity in key parameters [36], including adsorption rates and the LORO threshold. Such biological noise would desynchronize cell lysis events, leading to a broader, more gradual collapse curve. Single-cell measurements of adsorption rate distributions and superinfection thresholds would help refine our understanding of synchronized LINC.

Another effect that could contribute to the synchronicity of the dynamics

is spatial heterogeneity, such as the formation of host aggregates. Structured populations can strongly influence phage-bacteria interactions, even when aggregates are loose and well-mixed with phages at the population level [5, 37]. This study highlights the role of LO and LORO in dense colonies, but it remains an interesting future direction to investigate how LO and LORO operate in looser structures, such as small clusters or bacterial chains, where local MOI and spatial coupling may differ.

In summary, our individual-based model captures key dynamics of phage T4 infection, including timing fluctuations and MOI-dependent lysis phenomena such as LO, LIN, and LORO, which is difficult to take into account in concentration-based models [17]. Future experimental validation, particularly through single-cell approaches, will be crucial for deepening our understanding of phage-host interactions and refining predictive models of phage epidemics in bacterial communities.

Acknowledgement

ChatGPT (OpenAI) was used solely for language editing and improving readability. All content and interpretations are the responsibility of the authors. This research was funded by the Novo Nordisk Foundation (NNF21OC0068775).

References

[1] B. Koskella, M. A. Brockhurst, Bacteria-phage coevolution as a driver of ecological and evolutionary processes in microbial communities, FEMS Microbiol. Rev. 38 (5) (2014) 916–931.

[2] C. H. Wigington, D. Sonderegger, C. P. D. Brussaard, A. Buchan, J. F. Finke, J. A. Fuhrman, J. T. Lennon, M. Middelboe, C. A. Suttle, C. Stock, W. H. Wilson, K. E. Wommack, S. W. Wilhelm, J. S. Weitz, Re-examination of the relationship between marine virus and microbial cell abundances, Nat. Microbiol. 1 (3) (2016) 15024.

[3] B. P. Taylor, C. J. Penington, J. S. Weitz, Emergence of increased frequency and severity of multiple infections by viruses due to spatial clustering of hosts, Phys. Biol. 13 (6) (2017) 066014.

[4] R. S. Eriksen, S. L. Svenningsen, K. Sneppen, N. Mitarai, A growing microcolony can survive and support persistent propagation of virulent phages, Proceedings of the National Academy of Sciences 115 (2) (2018) 337–342.

[5] R. S. Eriksen, N. Mitarai, K. Sneppen, On phage adsorption to bacterial chains, Biophys. J. 119 (9) (2020) 1896–1904.

[6] N. Visconti, Resistance to lysis from without in bacteria infected with t2 bacteriophage1, J. Bacteriol. 66 (3) (1953) 247–253.

[7] R. Young, Bacteriophage lysis: mechanism and regulation, Microbiol. Rev. 56 (3) (1992) 430–481.

[8] S. T. Abedon, Lysis of lysis-inhibited bacteriophage T4-infected cells, J. Bacteriol. 174 (24) (1992) 8073–8080.

[9] A. H. Doermann, Lysis and lysis inhibition with escherichia coli bacteriophage, J. Bacteriol. 55 (2) (1948) 257–276.

[10] R. Josslin, The lysis mechanism of phage T4: mutants affecting lysis, Virology 40 (3) (1970) 719–726.

[11] S. T. Abedon, Look who's talking: T-even phage lysis inhibition, the granddaddy of virus-virus intercellular communication research, Viruses 11 (10) (Oct. 2019).

[12] I. N. Wang, D. L. Smith, R. Young, Holins: the protein clocks of bacteriophage infections, Annu. Rev. Microbiol. 54 (2000) 799–825.

[13] E. S. Miller, E. Kutter, G. Mosig, F. Arisaka, others, Bacteriophage T4 genome, Microbiology (2003).

[14] R. Young, Phage lysis: do we have the hole story yet?, Curr. Opin. Microbiol. 16 (6) (2013) 790–797.

[15] D. Mehner-Breitfeld, J. M. F. Schwarzkopf, R. Young, K. Kondabagil, T. Brüser, The phage T4 antiholin RI has a cleavable signal peptide, not a SAR domain, Front. Microbiol. 12 (2021).

[16] S. T. Abedon, Selection for lysis inhibition in bacteriophage, J. Theor. Biol. 146 (4) (1990) 501–511.

[17] U. Hvid, N. Mitarai, Competitive advantages of T-even phage lysis inhibition in response to secondary infection, PLoS Comput. Biol. 20 (7) (2024) e1012242.

[18] W. Bode, Lysis inhibition in escherichia coli infected with bacteriophage T4, J. Virol. 1 (5) (1967) 948–955.

[19] N. Mitarai, S. Brown, K. Sneppen, Population dynamics of phage and bacteria in spatially structured habitats using phage and escherichia coli, J. Bacteriol. 198 (12) (2016) 1783–1793.

[20] V. Sinha, A. Goyal, S. L. Svenningsen, S. Semsey, S. Krishna, In silico evolution of lysis-lysogeny strategies reproduces observed lysogeny propensities in temperate bacteriophages, Front. Microbiol. 8 (2017) 1386.

[21] R. S. Eriksen, F. Larsen, S. L. Svenningsen, K. Sneppen, N. Mitarai, The dynamics of phage predation on a microcolony, Biophys. J. 123 (2) (2024) 147–156.

[22] A. Singh, J. J. Dennehy, Stochastic holin expression can account for lysis time variation in the bacteriophage , J. R. Soc. Interface 11 (95) (2014) 20140140.

[23] D. Gillespie, Approximate accelerated stochastic simulation of chemically reacting systems, Journal of Chemical Physics 115 (2001) 1716–1733.

[24] M. De Paepe, F. Taddei, Viruses' life history: towards a mechanistic basis of a trade-off between survival and reproduction among phages, PLoS Biol. 4 (7) (2006) e193.

[25] H. Hadas, M. Einav, I. Fishov, A. Zaritsky, Bacteriophage T4 development depends on the physiology of its host escherichia coli, Microbiology 143 (Pt 1) (1997) 179–185.

[26] A. Rabinovitch, I. Fishov, H. Hadas, M. Einav, A. Zaritsky, Bacteriophage T4 development in escherichia coli is growth rate dependent, J. Theor. Biol. 216 (1) (2002) 1–4.

[27] S. T. Abedon, Lysis from without, Bacteriophage 1 (1) (2011) 46–49.

[28] J. Hu, K. Miyanaga, Y. Tanji, Diffusion properties of bacteriophages through agarose gel membrane, Biotechnol. Prog. 26 (5) (2010) 1213–1221.

[29] S. Heilmann, K. Sneppen, S. Krishna, Coexistence of phage and bacteria on the boundary of self-organized refuges, Proc. Natl. Acad. Sci. U. S. A. 109 (31) (2012) 12828–12833.

[30] J. J. Bull, K. A. Christensen, C. Scott, B. R. Jack, C. J. Crandall, S. M. Krone, Phage-bacterial dynamics with spatial structure: Self organization around phage sinks can promote increased cell densities, Antibiotics (Basel) 7 (1) (Jan. 2018).

[31] R. S. Eriksen, S. L. Svenningsen, K. Sneppen, N. Mitarai, A growing microcolony can survive and support persistent propagation of virulent phages, Proc. Natl. Acad. Sci. U. S. A. 115 (2) (2018) 337–342.

[32] E. Tzipilevich, M. Habusha, S. Ben-Yehuda, Acquisition of phage sensitivity by bacteria through exchange of phage receptors, Cell 168 (1-2) (2017) 186–199.e12.

[33] R. Young, Phage lysis: three steps, three choices, one outcome, J. Microbiol. 52 (3) (2014) 243–258.

[34] J. J. Dennehy, I.-N. Wang, Factors influencing lysis time stochasticity in bacteriophage , BMC Microbiol. 11 (1) (2011) 174.

[35] C. Wedd, T. Yunusov, A. Smith, R. Li, G. Hardo, M. Hunter, R. Majed, D. Fusco, S. Bakshi, Single-cell imaging of the lytic phage life cycle in bacteria, bioRxiv (2024) 2024.04.11.588870.

[36] C. Igler, Phenotypic flux: The role of physiology in explaining the conundrum of bacterial persistence amid phage attack, Virus Evol 8 (2) (2022) veac086.

[37] A. Yadav, N. Mitarai, K. Sneppen, Self-organized coexistence of phage and a population of host colonies, bioRxiv (2024) 2024.09.02.610744.